6. G. S. Park, S. Y. Park, R. H. Kyser, C. M. Armstrong, A. K. Ganguly, and R. K. Parker, Broadband Operation of a Ka-Band Tapered Gyro-Traveling-Wave Amplifier, *IEEE Trans. Plasma Sci.*, Vol. PS-22, 1994, pp. 536–543.
7. H. S. Uhm, J. Y. Choe, and S. Ahn, "Theory of Gyrotron Amplifier in a Waveguide with Inner Dielectric Material," *Int. J. Electron.*, Vol. 51, 1981, pp. 521–532.
8. S. J. Rao, P. K. Jain, and B. N. Basu, Two-Stage Dielectric-Loading for Broadbanding a Gyro-TWT, *IEEE Electron Device Letters*, Vol. EDL-17, 1996, pp. 303–305.
9. S. J. Rao, P. K. Jain, and B. N. Basu, "Broadbanding of a Gyro-TWT by Dielectric-Loading through Dispersion Shaping," *IEEE Trans. Electron Devices*, to be published.
10. H. S. Uhm and J. Y. Choe, "Properties of the Electromagnetic Wave Propagation in a Helix-Loaded Waveguide," *J. Appl. Phys.*, 1982, Vol. 53, pp. 8483–8488.
11. H. S. Uhm and J. Y. Choe, "Electromagnetic-Wave Propagation in a Conducting Waveguide Loaded with a Tape Helix," *IEEE Trans. Microwave Theory Tech.*, Vol. MTT-31, 1983, pp. 704–709.
12. H. S. Uhm and J. Y. Choe, "Theory of Gyrotron Amplifier in a Helix Loaded Waveguide," *J. Appl. Phys.*, Vol. 54, 1983, pp. 4889–4894.
13. S. Ghosh, P. K. Jain, and B. N. Basu, "Fast-Wave Analysis of an Inhomogeneously-Loaded Helix Enclosed in a Cylindrical Waveguide," *IEEE Trans. Microwave Theory Tech.*, to be published.
14. S. J. Rao, P. K. Jain, and B. N. Basu, "Hybrid-Mode Helix-Loading Effects on Gyro-Traveling-Wave Tubes," *Int. J. Electron. (UK)*, to be published.
15. S. Sensiper, "Electromagnetic Wave Propagation on Helical Structures," *Proc. IRE*, Vol. 43, 1955, pp. 149–161.
16. J. R. Pierce, *Traveling-Wave Tubes*, Van Nostrand, New York, 1950.

CCC 0895-2477/97

MODELING AND MEASUREMENT OF 2.44-GHz RADIO OUT-OF-SIGHT PROPAGATION ON SINGLE FLOORS

T. R. Liu[1] and J. H. Tarng[1]
[1]Department of Communication Engineering
National Chiao-Tung University
Hsinchu, Taiwan, Republic of China

Received 11 July 1996

ABSTRACT: *An easy-to-use DTR model combined with a patched-wall model is proposed to predict the path loss for out-of-sight propagation on a single floor through interior walls. The model demonstrates an accurate prediction, and is verified by comparison of the predicted path loss with the measured one of 2.44-GHz radio propagation at four different sites.* © *1997 John Wiley & Sons, Inc.* Microwave Opt Technol Lett 14, 56–59, 1997.

Key words: *indoor radio propagation modeling; radio measurement*

I. INTRODUCTION

There have been a number of recent investigations on indoor radio propagation modeling [1–9] because of its practical importance for wireless local area networks and personal communication networks [10, 11]. These articles have developed both empirically based statistical models [1–5] and theoretical models [6–9]. In Reference [6], the authors used absorbing screens to calculate the excess loss in offices. In Reference [7], the authors have developed a site-specific model by using the ray-tracing method to predict propagation based on blueprint representation. The concept of effective building material properties is developed.

In this article, a direct-transmitted ray (DTR) model combined with a patched-wall model [12] is proposed to predict the path loss for out-of-sight (OOS) propagation on single floors in office buildings if the direct-transmitted path is not blocked by metallic objects. Our model is not only easy to use, but also is reasonably accurate. The predicted path loss is compared with the measured one of 2.44-GHz radio propagation at four different sites.

Contract grant sponsor: National Science Council of Taiwan; Contract grant number: NSC 85-2221-E-009-35.

II. MEASUREMENT SETUP AND EXPERIMENTAL SITES

A. Measurement Setup and Procedure. Narrow-band (CW) signal strength measurements were made at 2.44 GHz. A 0- or 13-dBm CW signal was transmitted by a half-wavelength dipole antenna at a height 1.6 m above the ground. The transmitting system, including a signal generator, a section of cable, and the transmitting antenna, has been calibrated in an anechoic chamber to measure the 1-m transmitting field strength in free space. The receiving antenna is also a half-wavelength dipole antenna (Anritsu MP663A) with the same height. Both the transmitting and receiving antennas are vertically polarized during the measurement. The receiver (Advantest R3261A) can instantaneously measure the signal strength between 0 and -110 dBm over 10 kHz for 2.44 GHz. The value of the received power is acquired automatically by a personal computer with a GPIB card. At each measured position, the measured field strength is obtained by a spatial sector average over nine grid subpoints with a quarter-wavelength spacing between neighboring subpoints. To assure that the propagation channel is time stationary during the measurement, the measured data have been averaged on screen over 10 instantaneous sampled values.

B. Experimental Sites and Patched-Wall Models. Measurements were made at four different sites, which are all located on the ninth floor of Engineering Building Four at the National Chiao-Tung University in Hsin-Chu. Figure 1 shows the layout of site No. 1. The walls of room 911A are made of

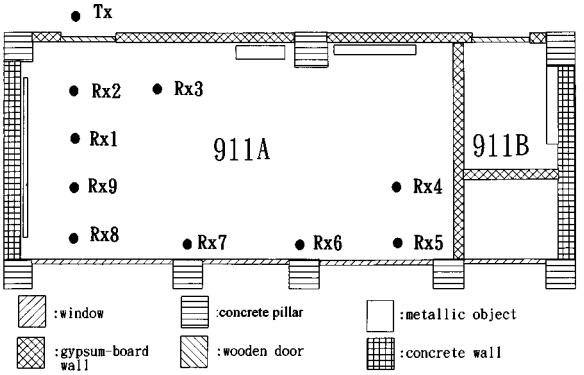

Figure 1 Layout of measurement site No. 1. There are nine receiving positions. Several patches are used to form the walls of room 911A ($9 \times 10 \times 3$ m)

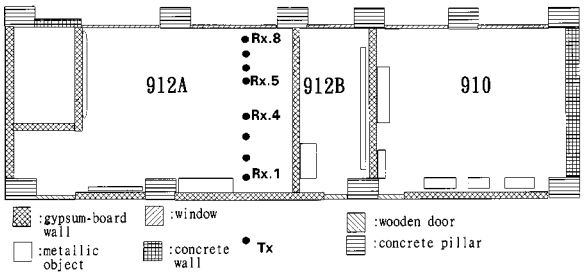

Figure 2 Layout of measurement site No. 2. There are eight receiving positions. The patched-wall model is used to describe the surrounding walls of the receiving positions, which is at room 912A ($8 \times 6 \times 3$ m)

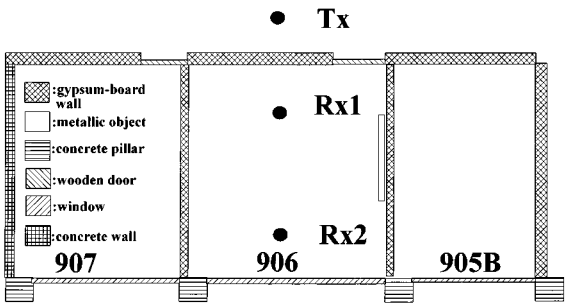

Figure 3 Layout of measurement site No. 3. There are two receiving positions. The size of room 906 ($7 \times 3 \times 3$ m) is smaller than other sites

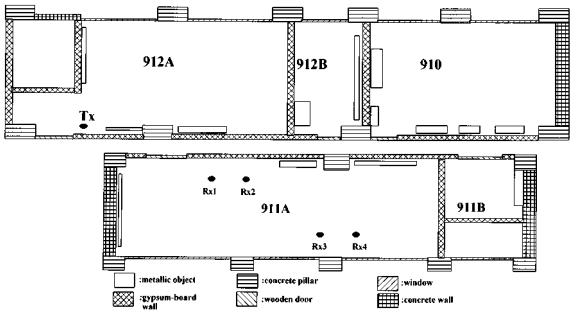

Figure 4 Layout of measurement site No. 4. The transmitting and receiving antennas are in two different rooms, room 912A ($8 \times 6 \times 3$ m) and 911A ($9 \times 10 \times 3$ m)

gypsum board or concrete. A patched-wall model is employed to describe and shape the surrounding walls of the receiving positions by introducing patches of different sizes and dielectric constants. These patches are used to represent the surfaces of gypsum-board walls, concrete walls, or wooden doors. The dimensions and dielectric constants of each patch are decided, respectively, by the physical size and the material it represents. There are some metallic objects, such as an air conditioner, file cabinets, bookcases, and blackboards, in room 911A, as shown. These metallic objects may block the direct-transmitted ray. T_x and R_{xi} represent the positions of the transmitting and receiving antennas, respectively, where $i = 1, \ldots, 9$. In Figures 2–4 the layouts of measurement site Nos. 2–4 are illustrated, respectively. In each measurement site the patched-wall model is used to shape the surrounding walls. To verify the DTR model, the receiving positions are properly chosen so that the direct-transmitted path is not blocked by the metallic objects at each site.

For all the measurements, the transmitting antenna is held stationary and placed in a corridor or an office room, and the receiving antenna is placed at different locations in the rooms.

III. PROPAGATION MODEL AND COMPARISONS

A. Propagation Model. For radio-wave propagation in indoor environments many researchers have employed a two-dimensional ray-tracing method to determine the received field strength [6, 7]. Many rays, such as direct, transmitted, reflected, and multiply transmitted or reflected rays, are traced and to see whether they are received or not. In our study, only a direct-transmitted (-refracted) ray (if exists) is traced and used to compute the average path loss for OOS propagation. This direct-transmitted ray (DTR), determined by the principle of geometric optics, may experience transmissions (refractions) more than once before it arrives at the receiving antenna. The complex received field is given by

$$E_R = E_0 G_t G_r L(d) \prod_i T(\theta_i), \tag{1}$$

where E_0 is the field in free space 1 m away from the transmitting antenna, and G_t and G_r are the field-amplitude radiation gains of the transmitting and the receiving antennas, respectively. $L(d)$ is the free-space path loss with a total path length d. $T(\theta_i)$ is the transmission coefficient of the ray with incident angle θ_i propagating through the ith patched wall, which stands between the transmitting and receiving antennas. In our model, the structure of the wall is considered to be multilayered, and the transmission coefficient $T(\theta_i)$ is calculated by the $ABCD$ matrix and is given by [13]

$$T(\theta_i) = \frac{2}{A + B/Z_t + Z_1(C + D/Z_t)}. \tag{2}$$

The notations A, B, C, and D are computed by

$$\begin{bmatrix} A & B \\ C & D \end{bmatrix} = \begin{bmatrix} A_1 & B_1 \\ C_1 & D_1 \end{bmatrix} \begin{bmatrix} A_2 & B_2 \\ C_2 & D_2 \end{bmatrix} \cdots \begin{bmatrix} A_N & B_N \\ C_N & D_N \end{bmatrix}. \tag{3}$$

Coefficients in each matrix on the right-hand side of the equation above is determined by dielectric constant, permeability, layered thickness, and refractive angle of the corresponding layer. For example, for layer m,

$$A_m = D_m = \cos q_m l_m, \qquad B_m = jZ_m \sin q_m l_m, \qquad m = 1, \ldots, N, \tag{4}$$

$$C_m = \frac{j \sin q_m l_m}{Z_m}, \qquad A_m D_m - B_m C_m = 1, \tag{5}$$

$$q_m = k_m \cos \theta_m = k_m \left[1 - \left(\frac{n_1}{n_m}\right)^2 \sin^2 \theta_i\right]^{1/2}, \qquad k_m = k_0 \cdot n_m, \tag{6}$$

where θ_m is the refractive angle. Notation l_m is the layer thickness and n_m is the index of refraction. k_0 is the free-space wave number. It is noted that $z_m = \omega\mu_m/q_m$.

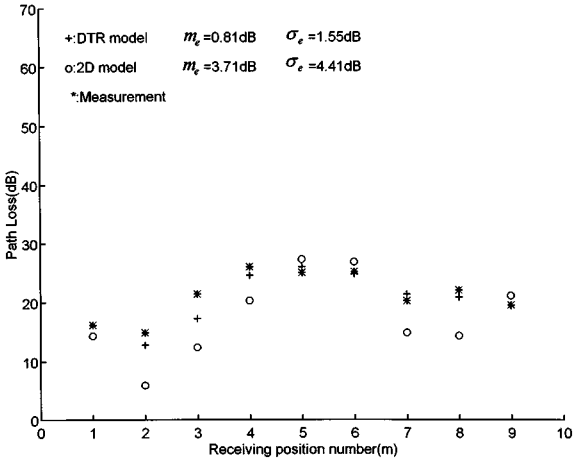

Figure 5 The measured and predicted path losses of 2.44 GHz for receiving positions at measurement site No. 1. The predicted path loss is computed by the DTR and 2D models

B. Numerical Simulations and Comparisons. In the numerical simulation made with the direct-transmitted ray (DTR) model, the dielectric constants of windows, gypsum-board walls, and concrete walls are chosen to equal 2.4, $5 - j0.062$ and $7 - j0.6$ [14, 15], respectively. To compare the computed path loss with the measured one at site No. 1, both the DTR model and a two-dimensional (2D) ray-tracing model are employed. The 2D ray-tracing model not only traces the direct-transmitted ray, but also includes multiply transmitted or reflected rays. Its algorithm and formulation can be found in Reference [7]. In Figure 5 it is found that the DTR model gives an accurate prediction with $m_e = 0.81$ dB and $\sigma_e = 1.55$ dB, where m_e represents the mean of the error and σ_e is the standard deviation of the error. This comparison shows that the direct-transmitted ray (if it exists) is the dominant path for OOS propagation in an indoor environment. Those transmitted and reflected rays may give little contribution to the average received field strength. Figures 6–8 show the predicted path loss computed by the DTR model and the measured one at site Nos. 2–4, respectively. The DTR model still gives a consistent prediction accuracy with reasonable values of m_e and σ_e at different sites.

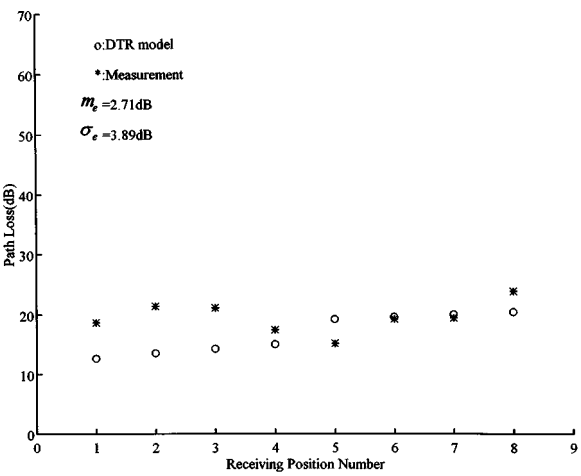

Figure 6 The measured and predicted path losses of 2.44 GHz for receiving positions at measurement site No. 2

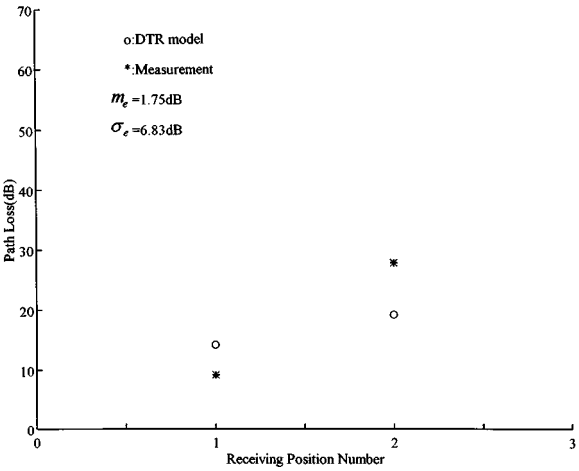

Figure 7 The measured and predicted path losses of 2.44 GHz for receiving positions at measurement site No. 3

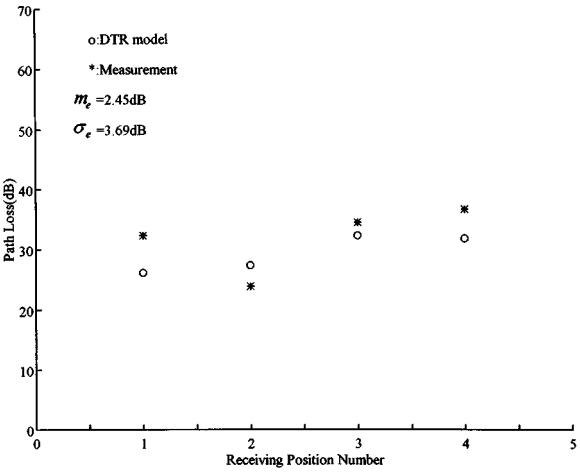

Figure 8 The measured and predicted path losses of 2.44 GHz for receiving positions at measurement site No. 4

V. CONCLUSION

An easy-to-use and reasonably accurate direct-transmitted ray model is proposed to predict the path loss for out-of-sight propagation on single floors in office buildings if the directed-transmitted path is not blocked by metallic objects. In this situation, the direct-transmitted ray (if it exists) is the dominant path, and those transmitted and reflected rays give little contribution to the average received field strength.

REFERENCES

1. S. Y. Seidel and T. S. Rappaport, "Path Loss Prediction in Multifloored Buildings at 914 MHz," *Electron. Lett.*, Vol. 27, July 1991, pp. 1384–1387.
2. S. Y. Seidel and T. S. Rappaport, "914 MHz Path Loss Prediction Models for Indoor Wireless Communications in Multifloored Buildings," *IEEE Trans. Antennas Propagat.*, Vol. AP-40, Feb. 1992, pp. 207–217.
3. A. J. Motley and J. M. P. Keenan, "Personal Communication Radio Coverage in Buildings at 900 MHz and 1700 MHz," *Electron. Lett.*, Vol. 24, June 1988, pp. 763–764.
4. A. J. Motley and J. M. P. Keenan, "Radio Coverage in Buildings," *British Telecommun. Technol. J.*, Special Issue on Mobile Communications, Vol. 8, 1990, pp. 19–24.

5. D. Molkdar, "Review on Radio Propagation into and within Buildings," *Proc. Inst. Elec. Eng., Pt. H*, Vol. 138, Feb. 1991, pp. 61–73.
6. W. Honcharenko, H. L. Bertoni, J. L. Dailing, J. Qian, and H. D. Yee, "Mechanisms Governing UHF Propagation on Single Floors in Modern Office Buildings," *IEEE Trans. Veh. Technol.*, Vol. VT-41, No. 4, 1992, pp. 496–504.
7. S. Y. Seidel and T. S. Rappaport, "Site-Specific Propagation Prediction for Wireless In-Building Personal Communication System Design," *IEEE Trans. Veh. Technol.*, Vol. VT-43, No. 4, 1994, pp. 879–892.
8. G. M. Whitman, K. S. Kim, and E. Niver, "A Theoretical Model for Radio Signal Attenuation inside Buildings," *IEEE Trans. Veh. Technol.*, Vol. 44, No. 3, 1995, pp. 621–629.
9. A. Kajiwara, "Line-of-Sight Indoor Radio Communication Using Circular Polarized Waves," *IEEE Trans. Veh. Technol.*, Vol. 44, No. 3, Aug. 1995, pp. 487–493.
10. Marcus, "Regulatory Policy Considerations for Radio Local Area Networks," *IEEE Communications Magazine*, Vol. 25, No. 7, July 1987, pp. 95–99.
11. H. Hashemi, "The Indoor Radio Propagation Channel," *Proc. IEEE*, Vol. 81, No. 7, 1993, pp. 943–968.
12. B. J. Hsu, J. H. Tarng, and W. J. Chang, "Modeling and Measurement of 2.44 GHz and 900 MHz Radio Propagation in Corridors," *Conf. Record of ICUPC'95*, pp. 188–191.
13. Akira Ishimaru, *Electromagnetic Wave Propagation, Radiation, and Scattering*, Prentice-Hall, Englewood Cliffs, NJ, 1991.
14. C. F. Yang, C. J. Ko, and J. Y. Chen, "Measurement of the Dielectric Constants of the Walls in Buildings," *Proceedings of the 1st Radio Science Symposium*, Kaohsiung, Taiwan, 1995, pp. 63–67.
15. M. C. Lawton and J. P. McGeehan, "The Application of a Deterministic Ray Launching Algorithm for the Prediction of Radio Channel Characteristic in Small-Cell Environments," *IEEE Trans. Veh. Technol.*, Vol. VT-43, No. 4, 1994, pp. 966–969.

CCC 0895-2477/97

THE TRANSMISSION-LINE THEORY APPLIED TO OPTICAL FILTERS

Hosung Chang[1], and Je-Myung Jeong[1], and Sung Kyou Lim[2]
[1]Department of Radio Science and Engineering
Hanyang University
Seoul 133-791, Korea
[2]Department of Electronic Engineering
Dankook University
Cheonan, Korea

Received 22 July 1996

ABSTRACT: *A technique developed for tapered transmission lines is presented for the design of optical filters. Optical filters with graded index profiles are analyzed by solution of the nonlinear Riccati equation. Numerical results show that the method provides accurate solutions and computes the frequency response of the filters faster than the matrix method. © 1997 John Wiley & Sons, Inc.* Microwave Opt Technol Lett 14, 59–62, 1997.

Key words: *tapered lines; optical filters; graded index profiles*

I. INTRODUCTION

Recently the use of high-quality graded-index films as antireflection coatings on various optical devices, on narrow-band high rejection filters, and on nonpolarizing beam splitters [1] has garnered increased attention as the fabrication technology has developed. Graded-index layers (inhomogeneous layers) potentially provide less scattering, less stress, and better adhesion than step-index films (homogeneous layers) [2]. The matrix method [3] is extensively used to analyze homogeneous layers, and can also be utilized for the analysis of an inhomogeneous layer by dividing an inhomogeneous refractive index profile into a large number of homogeneous ones. Sossi [4] introduced the Fourier-transform method for the design of optical filters, and the method has been developed further by Verly and Dobrowolski [1], Bovard [5,], and Fabricius [7]. This Fourier-transform method, one of the design tools, generates continuous refractive index profiles corresponding to desired frequency spectra. In microwave studies, design techniques and analytical tools have been developed for multisection transformers and tapered transmission lines [8].

In this article we describe the analysis of an optical filter with a step-index profile, which can be considered as a multisection impedance transformer. We obtain reflection coefficients for normal and oblique incidence by calculating the input impedances at successive boundaries. We analyze graded index profiles by solving the nonlinear Riccati equation with the Runge–Kutta numerical method. An optical filter is designed by applying the Fourier transform to the Riccati equation, and the resultant graded index profile approaching to the target spectrum is obtained by repeating design procedures.

II. TRANSMISSION-LINE THEORY

A. Homogeneous Layers. We first consider two homogeneous layers, consisting of an incident medium and an exit medium, as shown in Figure 1(a), to discuss reflection and transmission of *s*-polarized waves from the boundaries of lossless media with a step-index profile. Assuming the field of the form

$$\mathbf{E}_i = E_0 e^{-j\beta(x \sin \theta_i + z \cos \theta_i)} \mathbf{a}_y, \tag{1}$$

we have the reflected field from Snell's law of reflection

$$\mathbf{E}_r = E_0 \Gamma_b e^{-j\beta(x \sin \theta_i - z \cos \theta_1)} \mathbf{a}_y, \tag{2}$$

where Γ_b is the reflection coefficient at the boundary and E_0 is the amplitude of the incident field. From Maxwell's equations and the boundary condition, Γ_b is found to be [9]

$$\Gamma_b = \frac{\eta_2 \cos \theta_1 - \eta_1 \cos \theta_2}{\eta_2 \cos \theta_1 + \eta_1 \cos \theta_2}, \tag{3}$$

where η_i is the intrinsic impedance of a medium. Reflection coefficient at a distance $z = -l$ away from the interface is given by

$$\Gamma(-l) = \frac{E_r(-l)}{E_i(-l)} = \Gamma_b e^{-j2\beta l \cos \theta_1}. \tag{4}$$